

Antikaons and higher order couplings in relativistic-mean field study of neutron stars

Neha Gupta and P. Arumugam

Department of Physics, Indian Institute of Technology Roorkee, Roorkee - 247 667, India

We investigate the role of higher order couplings, along with the condensation of antikaons (K^- and \bar{K}^0), on the properties of neutron star (NS). We employ extended versions of the relativistic mean-field model, in which kaon-nucleon and nucleon-nucleon interactions are taken on the same footing. We find that the onset of condensation of K^- and \bar{K}^0 highly depends not only on the strength of optical potential but also on the new couplings. The presence of antikaons leads to a softer equation of state and makes the neutron star core symmetric and lepton-deficient. We show that these effects strongly influence the mass-radius relation as well as the composition of neutron star. We also show that the recently observed 1.97 ± 0.04 solar mass NS can be explained in three ways: (i) a stiffer EoS with both antikaons, (ii) a relatively soft EoS with K^- and (iii) a softer EoS without antikaons.

PACS numbers: 26.60.-c, 26.60.Kp, 13.75.Jz, 97.60.Jd

I. INTRODUCTION

Neutron stars (NSs) are fascinating objects, attracting strong appeal as probes into the understanding of many areas of physics. The interior of a NS, where the density is very high, provides opportunities to apply and test the concepts of nuclear physics in order to elucidate properties such as NS mass and radius. These properties depend on the microscopic nature of the matter at high densities and can be corroborated with astrophysical observations [1–6].

In the recent years, several new observations have propelled several theories and a variety of models in a bid to understand the properties of NS [7–15]. In NS matter, while considering the conservation of only charge and baryon numbers, antikaons, hyperons and quarks can appear inside the NS by a strangeness changing process. At intermediate densities, pions and antikaons (K^- and \bar{K}^0) are most likely to condense. In a vacuum, pions are lighter than kaons, but this situation may be reversed in the dense medium due to strong interactions between mesons and nucleons [16, 17]. Hence antikaon condensation becomes more important in the intermediate density range and affects the mass and radius of the NS significantly.

As we approach the interior of the NS, density increases. The excitation energy of antikaons (strangeness = -1) decreases with density and hence at a sufficiently high density the antikaons are favoured to condense. Many theoretical descriptions have considered only the K^- condensation [18–24] which is supposed to be dominant as it occurs at a relatively low density. With the onset of K^- condensation, $n \rightarrow p + K^-$ is the most preferred process, and hence the proton fraction rises dramatically and even exceeds the neutron fraction at higher densities [24]. With the onset of \bar{K}^0 condensation this scenario will change completely. There will be a competition between the processes $N \rightarrow N + \bar{K}^0$ and $n \rightarrow p + K^-$, resulting in a perfectly symmetric matter of nucleons and antikaons inside the neutron stars [19].

A detailed study of the presence of antikaons, initially

proposed by Glendenning and Schaffner-Bielich [19], with relativistic mean-field (RMF) models has been carried out in [25–27]. In most of these previous works, the RMF parametrizations used were not tested rigorously in the case of finite nuclei. The recent parametrizations discussed in this work have been carefully developed and tested over the nuclear chart by explaining several nuclear properties [28–30] and the experimentally determined EoS for symmetric nuclear matter [10]. Hence, we are using more reliable models for the EoS which turn out to be softer (around the saturation density) than those used in the previous works. It is quite well-known that a softer EoS could lead to a lesser contribution from antikaons [26]. We have shown in our earlier work [24] that the EoS from recent parameterizations, with higher order couplings, is not too soft to neglect the role of antikaons. In such a case we have shown that the mixed phase (of kaonic and nonkaonic phases) will not appear due to the softer EoS. It has to be noted that it is not only the stiffness of EoS but also that of the symmetry energy that is crucial in determining the onset of antikaon condensation; hence their role in modifying the properties of NS. Some of the recent parameterizations (e.g. FSUG-old) yield very soft symmetry energies and its effect in altering onset of K^- and hence the properties of NS are discussed in our earlier work [24]. This study introspects our earlier conclusions with the inclusion of \bar{K}^0 which is a more realistic case [19].

For our calculations, we consider the effective field theory-motivated relativistic mean-field model (E-RMF) [31]. In this model, the idea of renormalizability is abandoned and the effective Lagrangian is expanded in powers of fields and its derivatives at a given order, with all the non-renormalizable couplings consistent with the underlying symmetries of QCD. In short, one can say that the E-RMF model comprises the standard RMF plus a few additional couplings. The RMF terms dominate at low density while the additional couplings dominate at high density. Without forcing any change in the parameters initially determined from a few magic nuclei [31], the E-RMF calculations explain finite nuclei and infinite matter

in a unified way with a commendable level of accuracy in both cases [10]. It is interesting to see how the E-RMF description of NS changes with the inclusion of antikaons, which is the central subject of this work.

In section II, we describe the Lagrangian, field equations and the expression for energy density followed by a discussion on the constraints for the antikaon condensation, with the parameters used. Our results and discussions are presented in section III which is followed by the conclusions drawn from present work.

II. THEORETICAL FRAMEWORK

The effective Lagrangian for the extended RMF models, after curtailing terms irrelevant to nuclear matter, can be written as

$$\begin{aligned} \mathcal{L} = & \bar{\psi} [g_\sigma \sigma - \gamma^\mu (g_\rho R_\mu + g_\omega V_\mu)] \psi \\ & + \frac{1}{2} \left(1 + \eta_1 \frac{g_\sigma \sigma}{m_n} + \frac{\eta_2}{2} \frac{g_\sigma^2 \sigma^2}{m_n^2} \right) m_\omega^2 V_\mu V^\mu \\ & + \left(1 + \eta_\rho \frac{g_\sigma \sigma}{m_n} \right) m_\rho^2 \text{tr}(R_\mu R^\mu) \\ & - m_\sigma^2 \sigma^2 \left(\frac{1}{2} + \frac{\kappa_3 g_\sigma \sigma}{3! m_n} + \frac{\kappa_4 g_\sigma^2 \sigma^2}{4! m_n^2} \right) \\ & + \frac{1}{4!} \zeta_0 g_\omega^2 (V_\mu V^\mu)^2, \end{aligned} \quad (1)$$

For the FSU2.1 model, the above Lagrangian has an additional term $\Lambda_v g_\rho^2 R_\mu \cdot R^\mu g_\omega^2 V_\mu V^\mu$. The symbols g_σ , g_ω , g_ρ , κ_3 , κ_4 , η_1 , η_2 , η_ρ , Λ_v and ζ_0 denote the various coupling constants. σ , V_μ , R_μ and ψ denote the scalar, vector and isovector meson fields and the nucleon field, respectively. m_σ , m_ω , and m_ρ are the corresponding meson masses and m_n is the nucleon mass. More details of the Lagrangian are explained explicitly in [13, 31].

The Lagrangian for the antikaon part reads

$$\mathcal{L}_K = D_\mu^* K^* D^\mu K - m_K^{*2} K^* K, \quad (2)$$

with $K \equiv K^-$ or \bar{K}^0 and is added to the E-RMF Lagrangian. The scalar and vector fields are coupled to antikaons in a way analogous to the minimal coupling scheme [19] via the relations

$$m_K^* = m_K - g_{\sigma K} \sigma \quad \text{and} \quad (3)$$

$$D_\mu = \partial_\mu + i g_{\omega K} V_\mu + i g_{\rho K} \tau_3 \cdot R_\mu, \quad (4)$$

where m_K stands for the antikaon's mass ($m_{K^-} = m_{\bar{K}^0} = 495$ MeV). Note that in the mean-field approximation, the fields σ , V_μ and R_μ are replaced by their expectation values σ , V_0 , and R_0 , respectively. In the presence of antikaons the coupling constants corresponding to these fields are represented by $g_{\sigma K}$, $g_{\omega K}$ and $g_{\rho K}$.

Energy relations for the antikaons (K^-, \bar{K}^0) are

$$\omega_{K^-, \bar{K}^0} = m_K - g_{\sigma K} \sigma - g_{\omega K} V_0 \mp g_{\rho K} R_0, \quad (5)$$

where \mp sign represents the isospin projection of antikaons K^- and \bar{K}^0 respectively. The expression for the energy of antikaons is linear in the meson field and represents that, with the increase of density, the energy of antikaons will decrease. The above expression also suggests that antikaon condensation is significantly influenced by the rho meson field or vice-versa.

In the presence of antikaons, the meson fields are given by

$$\begin{aligned} m_\sigma^2 \sigma = & g_\sigma \rho_s - \frac{m_\sigma^2 g_\sigma \sigma^2}{m_n} \left(\frac{\kappa_3}{2} + \kappa_4 \frac{g_\sigma \sigma}{3! m_n} \right) \\ & + \eta_\rho \frac{g_\sigma}{2 m_n} m_\rho^2 R_0^2 + \frac{1}{2} \left(\eta_1 + \eta_2 \frac{g_\sigma \sigma}{m_n} \right) \frac{g_\sigma}{m_n} m_\omega^2 V_0^2 \\ & + g_{\sigma K} (\rho_{K^-} + \rho_{\bar{K}^0}), \end{aligned} \quad (6)$$

$$\begin{aligned} m_\omega^2 V_0 = & g_\omega (\rho_p + \rho_n) - \left(\eta_1 + \frac{\eta_2 g_\sigma \sigma}{2 m_n} \right) \frac{g_\sigma \sigma}{m_n} m_\omega^2 V_0 \\ & - \frac{1}{3!} \zeta_0 g_\omega^2 V_0^3 - g_{\omega K} (\rho_{K^-} + \rho_{\bar{K}^0}), \end{aligned} \quad (7)$$

$$\begin{aligned} m_\rho^2 R_0 = & \frac{1}{2} g_\rho (\rho_p - \rho_n) - \eta_\rho \frac{g_\sigma \sigma}{m_n} m_\rho^2 R_0 \\ & - g_{\rho K} (\rho_{K^-} - \rho_{\bar{K}^0}), \end{aligned} \quad (8)$$

where ρ_s is the scalar density given by

$$\rho_s = \frac{\gamma}{(2\pi)^3} \sum_{i=n,p} \int_0^{k_{fi}} d^3 k \frac{m_n^*}{(k^2 + m_n^{*2})^{1/2}}, \quad (9)$$

and γ is the spin-isospin degeneracy factor and is equal to 2 (for spin up and spin down).

The densities of antikaons can be written as,

$$\rho_{K^-, \bar{K}^0} = 2(\omega_{K^-, \bar{K}^0} + g_{\omega K} V_0 \pm g_{\rho K} R_0) K^* K. \quad (10)$$

In NS matter only baryon number and the charge number are conserved, hence the constraints involving chemical potentials and baryon densities can be written as

$$\begin{aligned} \mu_n &= \mu_p + \mu_e, \\ \mu_e &= \mu_\mu, \quad \text{and} \\ q &= \rho_p - \rho_e - \rho_\mu - \rho_{K^-}. \end{aligned} \quad (11)$$

The energy density can be written as

$$\epsilon = \epsilon_N + \epsilon_{K^-, \bar{K}^0}, \quad (12)$$

where ϵ_N is the energy density of nucleon phase as given in Ref. [24]. The energy density contributed by antikaon condensation is

$$\epsilon_{K^-, \bar{K}^0} = m_K^* (\rho_{K^-} + \rho_{\bar{K}^0}). \quad (13)$$

Unlike the energy density, pressure is not directly affected by the inclusion of antikaons in an *s*-wave condensation

[19]. The conditions for onset of antikaons are $\omega_{K^-} = \mu_e$ for K^- and $\omega_{\bar{K}^0} = 0$ for \bar{K}^0 .

Calculational details for nucleon phase (n, p, e^-, μ^-) and the K^- phase (n, p, e^-, μ^-, K^-) have been discussed in [24]. For the \bar{K}^0 phase ($n, p, e^-, \mu^-, K^-, \bar{K}^0$), with the solution of the nucleon and the K^- phase in hand, we can calculate \bar{K}^0 energy from Eq. (5), which keeps decreasing as we increase the density. When the condition $\omega_{\bar{K}^0} = 0$ is first achieved, the \bar{K}^0 will occupy a small fraction of the total volume and the corresponding charge density, $q_{\bar{K}^0} \equiv 0$. We can calculate σ , V_0 , R_0 , k_{fp} , k_{fn} , k_{fe} , $k_{f\mu}$, ρ_{K^-} and $\rho_{\bar{K}^0}$, as in the K^- phase [24], with the condition $\omega_{\bar{K}^0} = 0$ for any chosen baryon density. After obtaining this solution we can calculate the energy density and pressure for the \bar{K}^0 phase. In our earlier calculations [24] with higher order couplings, we observed that the transition from the nucleon phase to the K^- phase is second order in nature. In such transitions the mixed phase, where the considered constituents can form a cluster, is not favoured.

For calculations using the E-RMF model with the inclusion of antikaons, we need two distinct sets of coupling constants: one being the nucleon-meson coupling constants and the other, the kaon-meson coupling constants. In the former case, the coupling constants are obtained by fitting to several properties of finite nuclei [31]. In this work we consider the parameter sets G1, G2 and FSU2.1. The FSU2.1 parameter set [13] has the same parameters as in the FSUGold parameter set [14] but has one extra term in the expression for pressure. The detailed list of parameters, for both kaon-meson and nucleon-meson couplings (G1, G2 and FSUGold), are given in [24].

III. RESULTS AND DISCUSSION

First, we look into the conditions at which the antikaons start to appear in the symmetric matter, neutron matter and NS matter. For this we calculate the antikaon energies ($\omega_{K^-}, \omega_{\bar{K}^0}$) along with difference in chemical potentials of neutrons and protons ($\mu_n - \mu_p$), corresponding to the considered matter. In Fig. 1, for a given matter, the point where ω_{K^-} crosses $\mu_n - \mu_p$ and the point at which $\omega_{\bar{K}^0} = 0$ represent the onset of K^- and \bar{K}^0 respectively. These calculations are with the G2 parameter set and $U_K = -120$ MeV. From Fig. 1, it is evident that at a particular density, ω_{K^-} increases while $\omega_{\bar{K}^0}$ decreases with the increase in neutron fraction. This difference is purely due to the contribution from the ρ field [Eq. (5)] and hence with a large neutron excess the K^- condensation is less favoured when compared to \bar{K}^0 . However, in neutron-rich matter, $\mu_n - \mu_p$ is larger and stiffer with density. This allows K^- to condense at lower densities.

Apart from the usual dependence on U_K , the onset of condensation of antikaons strongly depends on the parameters of the Lagrangian especially for the higher order couplings [24]. In case of K^- , this is due to the strong variation in the density dependence of ω_{K^-} and $\mu_n - \mu_p$

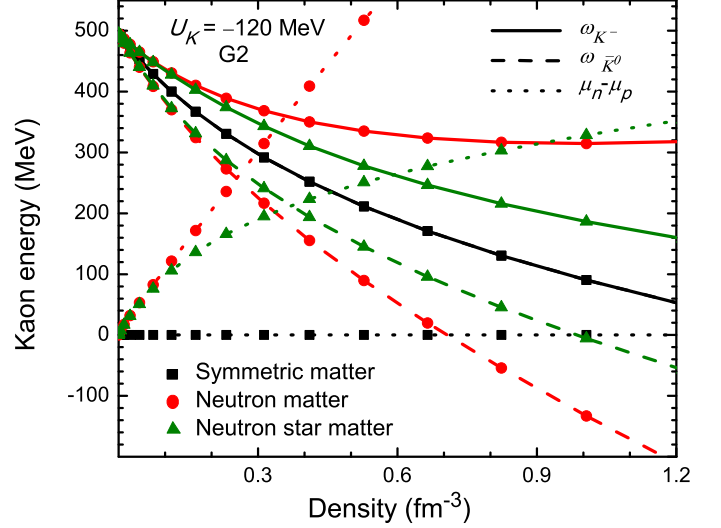


FIG. 1: Density dependence of the energies of antikaons and the difference of the calculated chemical potentials for the neutron and proton ($\mu_n - \mu_p$) for symmetric matter, neutron matter and NS matter. For a given matter, the point where ω_{K^-} crosses $\mu_n - \mu_p$ and the point at which $\omega_{\bar{K}^0} = 0$ represent the onset of K^- and \bar{K}^0 respectively. These calculations are done with the parameter set G2 with $U_K = -120$ MeV.

whose interplay determines the onset of K^- condensation. The density dependence of ω_{K^-} is similar to that of the EoS and $\mu_n - \mu_p$ varies in a way similar to the symmetry energy. So any change in the density dependence of EoS or that of the symmetry energy will affect the onset as well as the effect of K^- condensation. In general, \bar{K}^0 can appear only at densities higher than the one at which K^- condenses [19]. This is due to the fact that only with K^- condensation the proton population increases and with increasing density the matter becomes symmetric at a point where \bar{K}^0 can start to contribute. Thus the onset of \bar{K}^0 depends on the onset of K^- which in turn depends on the value of U_K and the higher order couplings.

With the G2 parameter set, the densities at which K^- and \bar{K}^0 sets in are (i) for neutron matter : 0.36 and 0.71 fm $^{-3}$, (ii) for NS matter: 0.59 and 0.98 fm $^{-3}$, and (iii) for symmetric matter: 1.5 and 1.5 fm $^{-3}$, respectively. In further discussions, we consider NS matter with G1, G2 and FSU2.1 parameter sets which represent different extensions of the RMF model.

In Figure 2, we present the scalar, vector and isovector fields along with the electron chemical potential as a function of density for NS matter calculated with $U_K = -120$ MeV and -160 MeV. The σ and ω fields are attractive for antikaons and their pattern is almost similar for all parameter sets. The ρ field is weaker in the case of FSU2.1 [Figs. 2 (c) and (f)] and it is almost constant (due to the additional coupling representing the strength of isoscalar-isovector mixing). As discussed earlier, the change in energies of antikaons from their symmetric matter value depends purely on the ρ field. Hence the energies of an-

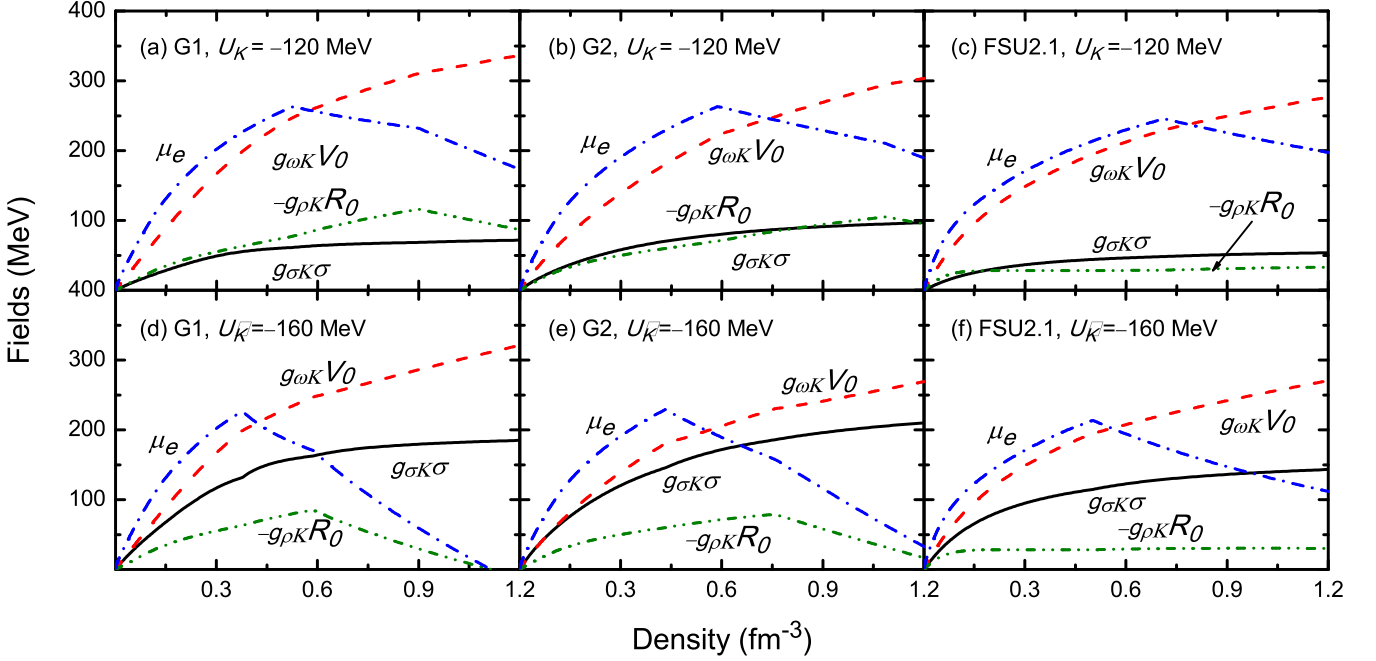


FIG. 2: The density dependence of the scalar ($g_{\sigma K \sigma}$), vector ($g_{\omega K} V_0$), and iso-vector ($-g_{\rho K} R_0$) fields in the NS matter inclusive of antikaon phase calculated with G1, G2 and FSU2.1 parameter sets for $U_K = -120$ MeV (top row) and -160 MeV (bottom row). The variation of electron chemical potential also is shown.

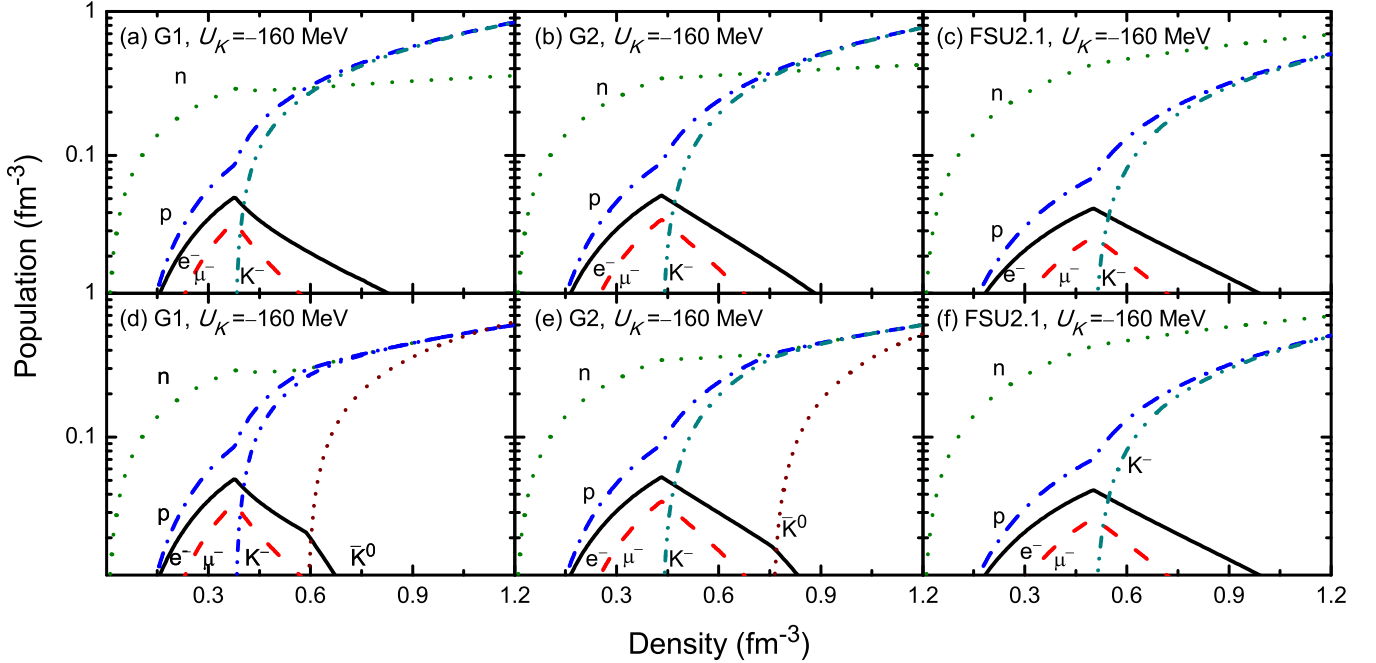


FIG. 3: The population of hadrons and leptons in NS matter as a function of baryon density calculated using different parameter sets (G1, G2, FSU2.1 shown in columns) with the inclusion of K^- (top row) and both K^- and \bar{K}^0 (bottom row) at $U_K = -160$ MeV.

tikaons in the case of FSU2.1 are not far from their symmetric matter values which will suppress the condensation of antikaons, especially the \bar{K}^0 . Due to this reason, with FSU2.1, the K^- condensation happens at a larger

density and the \bar{K}^0 does not appear at densities relevant to NS. In results with the G1 [Figs. 2 (a) and (d)], and G2 [Figs. 2(b) and (e)] parameter sets, as we increase density there are two kinks in μ_e . The first and second kinks

represent the onset of K^- and \bar{K}^0 condensation, respectively. After the first kink, the ρ field is enhanced due to the increased proton population with the $n \rightarrow p + K^-$ process. After the second kink, the ρ field is suppressed due to the equal population of protons and neutrons with the $N \rightarrow N + \bar{K}^0$ process which also suppresses the difference in K^- and \bar{K}^0 populations [Eq. (8)]. The sharpness in the kinks increase with the increases in the optical potential which also leads to the antikaon condensations at smaller densities while comparing Figs. 2(a) and (b) with Figs. 2(d) and (e), respectively.

In Figure 3, the population of different particles in NS is plotted against the baryon density, where the calculations are done using the G1, G2 and FSU2.1 parameters with optical potential $U_K = -160$ MeV. Results are given in the presence of only K^- [Figs. 3(a)-(c)] and with both K^- and \bar{K}^0 [Figs. 3(d)-(f)]. These results reflect all the features that we have discussed with the variation of different fields (Fig. 2). Calculations with G1, G2 parameter sets in the absence of \bar{K}^0 lead to a situation where the proton population exceeds that of neutron population [Figs. 3(a) and (b)]. This scenario changes once we include the \bar{K}^0 in our calculation [Figs. 3(d) and (e)], which suggests that the \bar{K}^0 starts to contribute at a density where the matter becomes symmetric ($\rho_p = \rho_n$). These results predict a symmetric NS core, where the population of both antikaons is almost same. Interestingly at higher density, the population of protons (or neutrons) and K^- are exactly the same. This means the negative charge is solely due to the K^- and hence no leptons are present. In case of our results with the FSU2.1 parameter set [Figs. 3(c) and (f)], K^- condenses at a higher density and hence \bar{K}^0 does not appear, even with $U_K = -160$ MeV. The delayed onset of K^- is due to the additional coupling as discussed earlier.

The calculated pressure versus energy density (EoS) for different cases is displayed in Fig. 4 where we observe the regular feature of exotic particles softening the EoS. With the onset of K^- the EoS become softer which is further softened with the onset of \bar{K}^0 . We observe that the EoS is strongly influenced by K^- whereas the \bar{K}^0 is important only at very high U_K . In the nucleon phase, G2 gives a softer EoS compared to G1 and FSU2.1 parameter sets. The EoS follows the same pattern after the inclusion of K^- and then \bar{K}^0 , with both $U_K = -120$ and -160 MeV. The sensitivity of EoS in the presence of antikaons, to the parameter U_K depends on the stiffness of symmetry energy. FSU2.1 has a softer symmetry energy and hence the corresponding EoS is not very sensitive to U_K .

The role of antikaons in modifying the EoS is very well-reflected in the results for the mass-radius relation of NS which are presented in Fig. 5 for different parameter sets at different values of U_K . These results are obtained by solving the well-known Tolman-Oppenheimer-Volkoff (TOV) equations [32, 33]. It is not always true that ‘earlier is the onset of antikaons, the greater their effect on the mass-radius relation’. The different factors

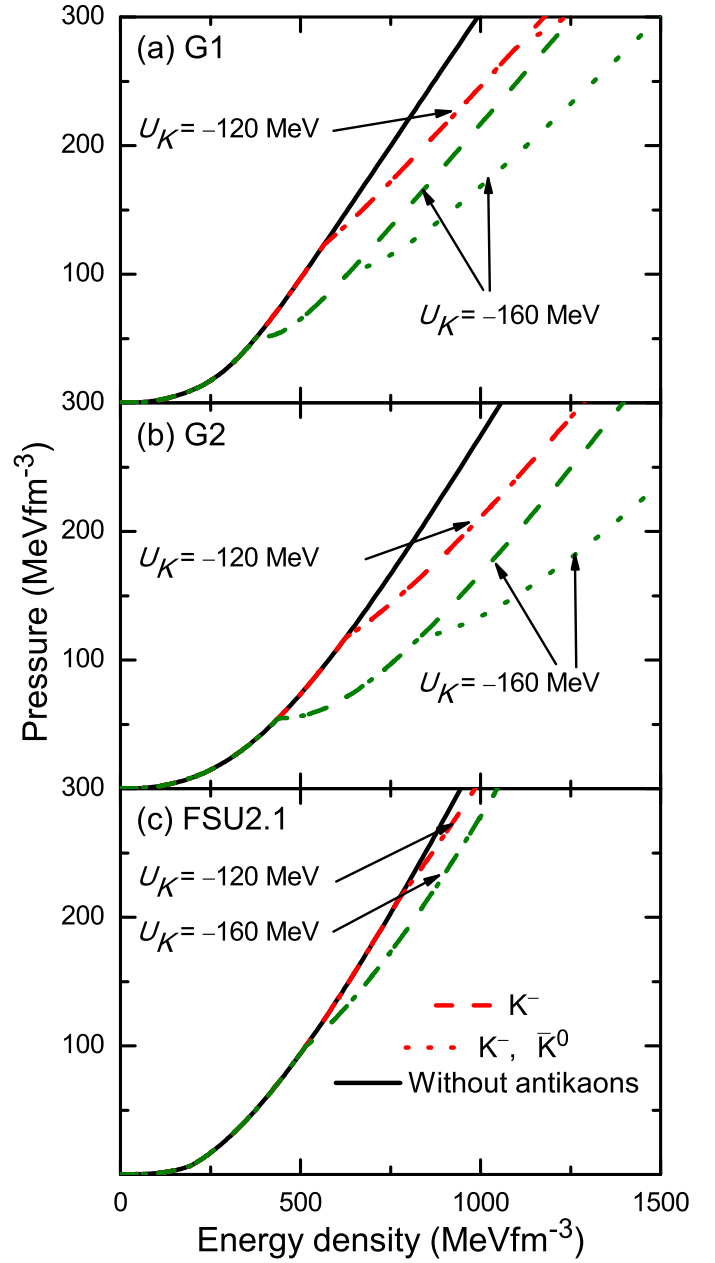


FIG. 4: The EoS for a nucleon (solid lines), K^- (dashed lines) and \bar{K}^0 (dotted lines) phases with (a) G1, (b) G2, and (c) FSU2.1 parameter sets.

governing the change in maximum mass in the presence of K^- are discussed in our previous work [24]. With the fact that the presence of \bar{K}^0 depends mostly on that of K^- , the influence of \bar{K}^0 on the mass-radius relation depends on the influence of K^- . Maximum mass with the G2 parameter set decreases with the inclusion of K^- at $U_K = -120$ MeV, where \bar{K}^0 does not contribute. With $U_K = -160$ MeV, there is a significant reduction of mass in the presence of K^- and the inclusion of \bar{K}^0 marginally decreases the mass further. We observe a similar trend in the case of G1 where both the antikaons play a stronger

role. With the FSU2.1 parameter set, the sensitivity of U_K to the EoS is less and hence the mass and radius changes marginally with the inclusion of K^- and the \bar{K}^0 does not play any role. All our results are quite consistent with the recent observations depicted in Fig. 5. It is interesting to note that the recently observed [6] pulsar PSR J1614-2230 of mass $1.97 \pm 0.04 M_\odot$ could be explained with three different compositions, namely (i) with both antikaons in case of G1, (ii) with K^- only in case of FSU2.1 and (iii) without antikaons in case of G2. It could be worthwhile to look into the details of these compositions.

Figure 6 represents the population of different particles in the NS versus the radial distance from the center of the NS, calculated with different parameter sets, when the NS has a maximum mass of approximately $2M_\odot$. We observe that without antikaons, the NS has a neutron-rich core and the presence of K^- makes it symmetric. With the onset of K^- , the population of leptons decrease drastically and this change depends on the value of U_K . In the case of FSU2.1, we need a large U_K which results in a negligible population of leptons in the core of the NS. Another interesting feature is the variation of radius of a $2M_\odot$ NS in the presence of antikaons. To accommodate such exotic particles at a fixed maximum mass (M), one should start with an EoS which is stiffer and yields a larger maximum mass without exotic particles. The presence of an exotic core reduces the maximum mass whereas the corresponding radius (R) may either increase or decrease. The antikaons can increase or decrease the central baryon density (ρ_c) [24] and hence R ($R \propto 1/\rho_c$), however only marginally. To accommodate more antikaons we need to start with a stiffer EoS yielding larger M and R , without antikaons. Thus for a given maximum mass, the corresponding radius is more if we have more antikaons (exotic particles). However, we may not observe stars extremely close to the maximum mass and hence the corresponding radius could vary. Hence more work is needed to understand the sensitivity of the radius of massive NS to the presence of exotic particles. In this work, we have ignored the presence of hyperons that can affect the role of antikaons and the NS properties. The onset of some of hyperons (Λ and Σ^-) can be in the same density range corresponding to the onset of antikaons. Hence the presence of hyperons can not only soften the EoS further but could cause a strong inter-

play between the hyperons and antikaons, affecting each other's role on the EoS. It will be interesting to study all these effects within the extended RMF models with higher order couplings. Work is in progress in this direction.

IV. CONCLUSIONS

With the inclusion of both antikaons (K^- and \bar{K}^0) in extended relativistic mean-field models (with parameter sets G1, G2 and FSU2.1), we observe that the onset of condensation of antikaons strongly depends on the kaon optical potential (U_K) and the parameters of the Lagrangian, especially the higher order couplings. This is similar to the conclusion in our earlier work [24] done only with the inclusion of K^- , where we attributed the onset as well as the effect of K^- condensation to the change in the density dependence of the EoS or that of symmetry energy. As \bar{K}^0 can appear only at densities higher than the one at which K^- condenses, the onset of \bar{K}^0 depends on the onset of K^- . With G1 and G2, we observe that the EoS is strongly influenced by K^- whereas the \bar{K}^0 is important only at higher U_K ($\gtrsim -140$ MeV). In case of the FSU2.1 parameter set, the additional higher order coupling softens the symmetry energy and hence the K^- condensation happens at a larger density and the \bar{K}^0 does not appear at densities relevant to the NS. These effects are well-reflected in the mass-radius relation and the composition of NS. The onset of \bar{K}^0 leads to symmetric and lepton-deficient matter at the core of the NS which would be proton-rich if we ignore \bar{K}^0 while the K^- dominates. We also observe that a $2M_\odot$ NS can be explained in three ways with: (i) a stiffer EoS with both antikaons, (ii) a relatively soft EoS with K^- and (iii) a softer EoS without antikaons. In the case of $2M_\odot$ being the maximum mass of an NS, we observe that greater concentration of antikaons leads to an increase in the radius (R_2) of such stars. Without antikaons (G2) we get $R_2 = 11.03$ km, with K^- (FSU2.1) we get $R_2 = 11.42$ km and with both K^- and \bar{K}^0 (G1) we get $R_2 = 12.55$ km. It would be interesting to study whether a precise information about the radius of massive NS could reveal the presence of exotic cores.

[1] D. J. Champion et al., *Science* **320**, 1309 (2008).
[2] S. M. Ransom et al., *Science* **307**, 892 (2005).
[3] P. C. C. Freire, A. Wolszczan, M. van den Berg, and J. W. T. Hessels, *Astrophys. J.* **679**, 1433 (2008).
[4] A. van der Meer, L. Kaper, M. H. van Kerkwijk, M. H. M. Heemskerk, and E. P. J. van den Heuvel, *Astron. Astrophys.* **473**, 523 (2007).
[5] T. Güver, P. Wroblewski, L. Camarota, and F. Özel, *Astrophys. J.* **719**, 1807 (2010).
[6] P. B. Demorest, T. Pennucci, S. M. Ransom, M. S. E. Roberts, and J. W. T. Hessels, *Nature* **467**, 1081 (2010).
[7] A. W. Steiner and S. Gandolfi, *Phys. Rev. Lett.* **108**, 081102 (2012).
[8] S. Gandolfi, J. Carlson, and S. Reddy, *Phys. Rev. C* **85**, 032801 (2012).
[9] A. W. Steiner, J. M. Lattimer, and E. F. Brown, *Astrophys. J.* **722**, 33 (2010).
[10] P. Arumugam, B. K. Sharma, P. K. Sahu, S. K. Patra,

T. Sil, M. Centelles, and X. Viñas, Phys. Lett. B **601**, 51 (2004).

[11] B. K. Sharma and S. Pal, Phys. Lett. B. **682**, 23 (2009).

[12] F. J. Fattoyev, C. J. Horowitz, J. Piekarewicz, and G. Shen, Phys. Rev. C **82**, 055803 (2010).

[13] G. Shen, C. J. Horowitz, and E. O'Connor, Phys. Rev. C **83**, 065808 (2011).

[14] B. G. Todd-Rutel and J. Piekarewicz, Phys. Rev. Lett. **95**, 122501 (2005).

[15] M. Hempel, T. Fischer, J. Schaffner-Bielich, and M. Liebendörfer, Astrophys. J **748**, 70 (2012).

[16] D. B. Kaplan and A. E. Nelson, Phys. Lett. B **175**, 57 (1986).

[17] S. Reddy, Acta Phys. Polon. B **33**, 4101 (2002).

[18] N. K. Glendenning, *Compact Stars* (Springer-Verlag, New York, 2007), 2nd ed.

[19] N. K. Glendenning and J. Schaffner-Bielich, Phys. Rev. C **60**, 025803 (1999).

[20] N. K. Glendenning, Phys. Rep. **342**, 393 (2001).

[21] G.-h. Wang, W.-j. Fu, and Y.-x. Liu, Phys. Rev. C **76**, 065802 (2007).

[22] T. Norsen and S. Reddy, Phys. Rev. C **63**, 065804 (2001).

[23] J. A. Pons, S. Reddy, P. J. Ellis, M. Prakash, and J. M. Lattimer, Phys. Rev. C **62**, 035803 (2000).

[24] N. Gupta and P. Arumugam, Phys. Rev. C **85**, 015804 (2012).

[25] S. Banik and D. Bandyopadhyay, Phys. Rev. C. **64**, 055805 (2001).

[26] S. Banik and D. Bandyopadhyay, Phys. Rev. C **63**, 035802 (2001).

[27] S. Pal, D. Bandyopadhyay, and W. Greiner, Nuclear Physics A **674**, 553 (2000).

[28] M. D. Estal, M. Centelles, and X. Viñas, Nucl. Phys. A **650**, 443 (1999).

[29] M. D. Estal, M. Centelles, X. Viñas, and S. K. Patra, Phys. Rev. C **63**, 024314 (2001).

[30] M. D. Estal, M. Centelles, X. Viñas, and S. K. Patra, Phys. Rev. C **63**, 044321 (2001).

[31] R. J. Furnstahl, B. D. Serot, and H.-B. Tang, Nucl. Phys. A **615**, 441 (1997).

[32] R. C. Tolman, Phys. Rev. **55**, 364 (1939).

[33] J. R. Oppenheimer and G. M. Volkoff, Phys. Rev. **55**, 374 (1939).

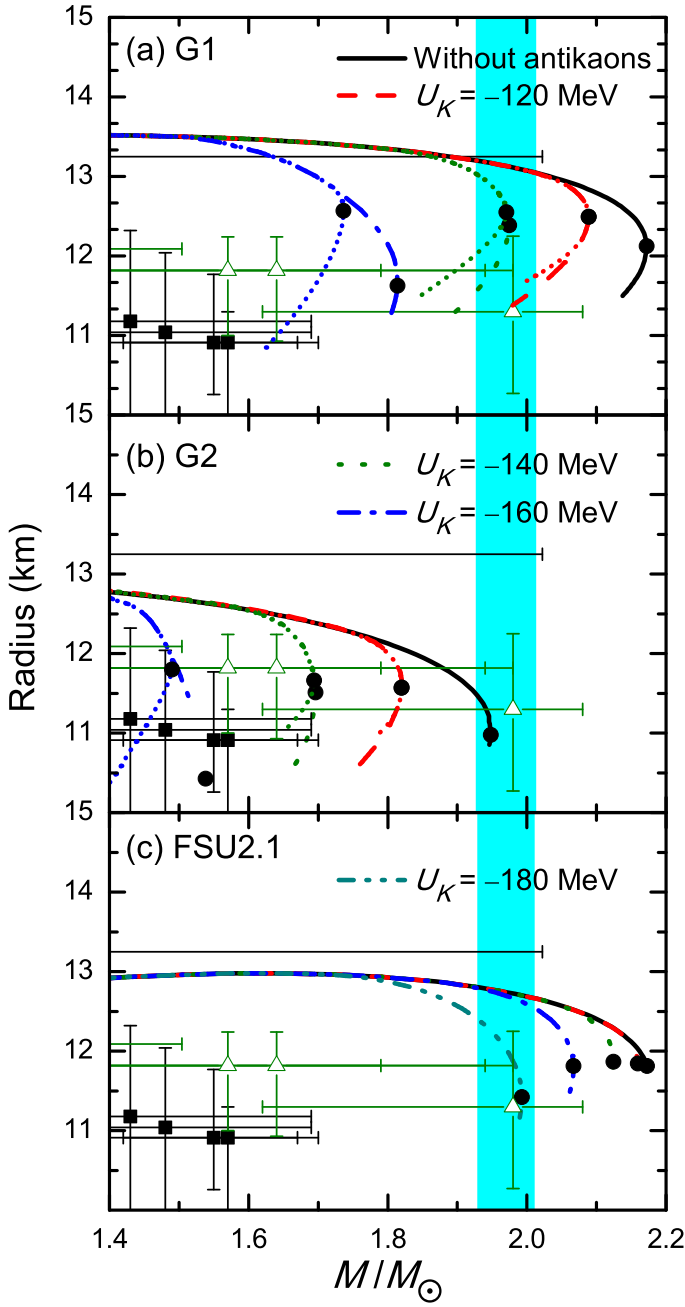


FIG. 5: The mass-radius relation from extended RMF models. Different curves represent the calculations using different kaon optical potentials (U_K) and with different parameter sets. For each parameter set, solid black line represents the pure nucleon phase, lines with different patterns and colors represent the phase with K^- and the corresponding small dotted lines represent the phase with both antikaons (K^-, \bar{K}^0). The different patterns and colors represent the strength of the kaon optical potential U_K ($|U_K|$ quantifies the influence of kaons) as specified in the inset. The solid circles represent the maximum mass in every case. Mass is given in units of solar mass M_\odot . Solid squares ($r_{ph} = R$) and open triangles ($r_{ph} \gg R$) represent the observational constraints [9], where r_{ph} is the photospheric radius. The shaded region corresponds to the recent observation of a $1.97 \pm 0.04 M_\odot$ star [6].

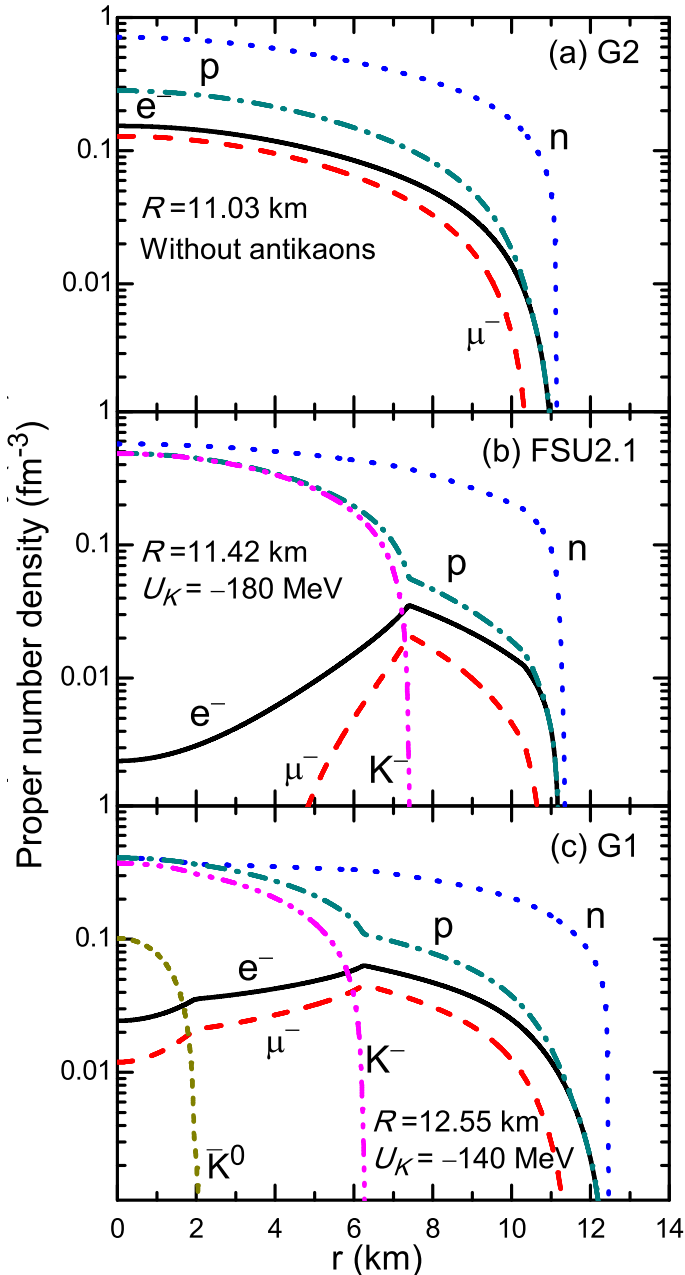


FIG. 6: The composition of an NS with a maximum mass of $2M_{\odot}$, calculated using G2, FSU2.1 and G1 parameter sets. The number density of various particles is plotted against the distance from the center of the NS. The values of U_K are adjusted to have the desired maximum mass.